Improved optical quality of GaNAsSb in the dilute Sb limit

Homan B. Yuen, Seth R. Bank, Mark A. Wistey, James S. Harris Jr., Maeng-Je Seong, Seokhyun Yoon, Robert Kudrawiec, and Jan Misiewicz

Citation: Journal of Applied Physics **97**, 113510 (2005); doi: 10.1063/1.1926398
View online: http://dx.doi.org/10.1063/1.1926398
View Table of Contents: http://scitation.aip.org/content/aip/journal/jap/97/11?ver=pdfcov
Published by the AIP Publishing

Improved optical quality of GaNAsSb in the dilute Sb limit

Homan B. Yuen,[a] Seth R. Bank, Mark A. Wistey, and James S. Harris, Jr.
Solid State and Photonics Laboratory, Department of Electrical Engineering, Stanford University, Stanford, California 94305-4075

Maeng-Je Seong[b] and Seokhyun Yoon[c]
National Renewable Energy Laboratory, 1617 Cole Boulevard, Golden, Colorado 80401

Robert Kudrawiec and Jan Misiewicz
Institute of Physics, Wroclaw University of Technology, Wybrzeze Wyspiańskiego 27, 50-370 Wroclaw, Poland

(Received 9 November 2004; accepted 5 April 2005; published online 25 May 2005)

GaNAs(Sb) layers were grown by solid-source molecular-beam epitaxy utilizing a radio frequency (rf) nitrogen plasma source. The samples contained less nitrogen and antimony (0.5%–0.8% N and $\leqslant$2% Sb) than in previous studies and were examined for their optical and electronic properties and any interactions between the elements. Secondary-ion-mass spectrometry, high-resolution x-ray diffraction, electroreflectance (ER) spectroscopy, and photoluminescence (PL) measurements were used to study those properties. We found that the addition of small amounts of antimony enhanced nitrogen incorporation into GaAs, similar to other studies that used 5–15$\times$ the mole fraction of antimony. The nitrogen concentration increased with increasing antimony flux. PL measurements indicated an improvement in optical quality with increasing nitrogen and antimony concentrations—contrary to the belief that adding more nitrogen necessarily degrades material quality. We collected and simulated ER spectra to examine the general band properties of the layers. Isoelectronic codoping can explain the improved quality when antimony is added to GaNAs. The improvement in GaNAs with small amounts of antimony holds great promise for improving strain-compensated GaInNAs(Sb)/GaNAs devices. © *2005 American Institute of Physics*. [DOI: 10.1063/1.1926398]

I. INTRODUCTION

The addition of nitrogen into InGaAs has enabled the growth of dilute-nitride materials that have much longer emission wavelengths than previously obtainable on GaAs.[1] Contrary to the behavior of most III-V semiconductors, small amounts of nitrogen in GaAs decrease both the overall lattice parameter and the band gap.[2] GaInNAs has enabled the development of lasers at the important fiber communication wavelength of 1.3 μm.[3–5] However, the incorporation of nitrogen into (In)GaAs is not without difficulty as the optical properties are degraded due to nonradiative traps, phase segregation, and/or relaxation.[6] These issues become more apparent in any attempts to add more indium and nitrogen to GaInNAs to reach technologically important wavelengths near 1.55 μm.[7] Antimony has been used in the past as a surfactant in semiconductor growth—improving the quality and surface of the material.[8] It was also used as a surfactant in GaInNAs growth to improve the material quality.[9,10] However, it was discovered that antimony acts as both a surfactant and constituent when employed during GaInNAs growth, forming GaInNAsSb.[7,11] Since antimony in GaAs also decreases the band gap, GaInNAsSb has allowed for the creation of devices out to 1.5 μm with the potential to reach 1.6 μm.[12,13] Although antimony improved GaInNAs material quality and surface morphology, it provided little improvement to indium-free GaNAs material; this may be due to the nature of antimony incorporation and the effects of adding indium. For the same flux of antimony, 2% antimony is found in GaInNAsSb while 8%–10% is found in GaNAsSb.[14] The change in antimony concentration is not primarily caused by a change in growth rates. This was confirmed by the growth of a GaInNAsSb sample and a GaNAsSb sample, grown with the same total group-III growth rate and antimony flux, that showed differing antimony concentrations. Therefore, it is indium that dramatically changes antimony incorporation between GaNAs and GaInNAs.

In this work, we examine the effects of adding small amounts of nitrogen and antimony to GaAs to study the interaction between the two elements. We show, using secondary-ion-mass spectrometry (SIMS), that the addition of even very small quantities of antimony enhances the incorporation of nitrogen. This result is similar to other studies which used 5–15$\times$ the amount of antimony.[14–16] High-resolution x-ray diffraction (HRXRD) results indicate very good, coherent epitaxial growth and interfaces. We obtained results from electroreflectance (ER) spectroscopy and simulated the spectra to examine the energy-band properties of the material. And finally, using photoluminescence (PL), we demonstrate an increase in PL intensity with increasing nitrogen and antimony concentrations of up to 2% antimony. This suggests that antimony, if used in the correct amounts,

[a]Electronic mail: hyuen@snow.stanford.edu
[b]Present address: Department of Physics, Chung-Ang University, Seoul, 156-756, South Korea.
[c]Present address: Division of Nano Sciences and Department of Physics, Ewha Womans University, Seoul 120-750, South Korea.

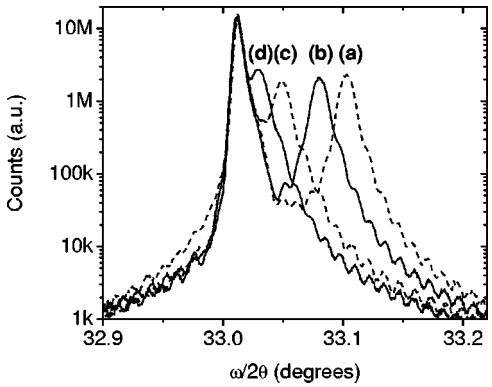

FIG. 1. (004) $\omega/2\theta$ HRXRD spectra of the four GaNAs(Sb) layers. (a) $GaN_{0.0063}As_{0.9937}$, (b) $GaN_{0.0071}As_{0.9869}Sb_{0.006}$, (c) $GaN_{0.008}As_{0.978}Sb_{0.014}$, and (d) $GaN_{0.0091}As_{0.9709}Sb_{0.02}$. The tensile strain decreases with increasing Sb flux.

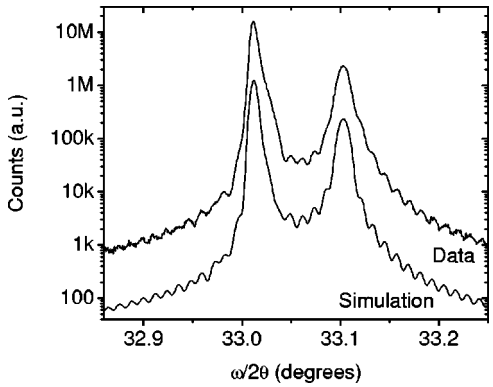

FIG. 2. (004) $\omega/2\theta$ HRXRD spectrum of the $GaN_{0.0063}As_{0.9937}$ sample with its corresponding simulated spectrum.

does improve the GaNAs material quality. The addition of antimony lifts the valence band, thus increasing hole confinement, and can be a useful band engineering component for the design of lasers.

II. EXPERIMENTAL DETAILS

The GaNAsSb samples used in this study were grown on *n*-type (100) GaAs substrates by solid-source molecular-beam epitaxy (MBE) in a Varian Mod. Gen-II system. Nitrogen was supplied by a modified SVT Associates plasma cell operating at a radio frequency (rf) of 13.56 MHz and 300 W forward power. A SUMO effusion cell was used to supply gallium. A valved arsenic cracker supplied As_2 and an unvalved antimony cracker supplied monomeric antimony. The GaNAsSb layers were grown at a substrate temperature of 425 °C, a growth rate of ~1.15 μm/h, and were 0.4 μm in thickness. An arsenic-to-gallium flux overpressure of 20×, an antimony flux of $1.0–2.8\times10^{-8}$-Torr beam equivalent pressure (BEP), and a nitrogen gas flow of 0.5 sccm (standard cubic centimeter per minute) were supplied during the growth. Four samples were grown under identical growth conditions except the antimony flux. The first sample was a GaNAs sample with 0.63% nitrogen and no antimony on top of a GaAs buffer layer. The next three samples were grown using the same procedures but included antimony fluxes of 1×10^{-8}, 2×10^{-8}, and 2.8×10^{-8}-Torr BEP, respectively.

III. RESULTS

The HRXRD (004) $\omega/2\theta$ scans, shown in Fig. 1, were used to examine structural quality and to measure the biaxial strain in the four GaNAs(Sb) layers. The nitrogen composition of the GaNAs sample was determined by dynamical simulation of the HRXRD spectra. The simulated spectrum of the GaNAs sample is shown in Fig. 2 with the real data for comparison. Simulations were also performed on the GaNAsSb spectra, but require SIMS for confirmation since quaternary compound compositions cannot be determined uniquely. All four samples have well-defined film diffraction peaks as well as distinct Pendellösung fringes. This suggests that all of the GaNAs(Sb) layers are coherent with the GaAs substrate, have good-quality interfaces, and have no discernible structural defects. Reciprocal space maps also indicated no phase segregation or relaxation had occurred. The (224) reciprocal space map for the GaNAsSb sample with 1.0×10^{-8}-Torr BEP Sb can be seen in Fig. 3. The other three space maps were very similar in appearance. As seen in Fig. 2, the strain of the GaNAs layer is tensile in nature as expected. With increasing antimony fluxes, the tensile strain decreases and approaches a lattice-matched condition in the GaNAsSb sample with 2.8×10^{-8}-Torr BEP antimony. The strain of the four samples was calculated from the position of the film diffraction peak and the results are shown in Table I.

SIMS was performed on the four samples to confirm and correlate the compositions with those obtained from HRXRD. The results for the antimony containing samples were used in conjunction with additional HRXRD simulations to refine the nitrogen values obtained from SIMS. The antimony concentration was known to a high degree of confidence since it was a straightforward analysis compared to nitrogen, which requires calibration. A summary of the results from those measurements is displayed in Table I. Although the same nitrogen flux was used for the GaNAs sample as for the other three, the amount of nitrogen in the layer increased with increasing antimony flux. The enhancement of nitrogen incorporation with antimony has been reported previously for larger antimony concentrations.[14–16] The effect is different in the present work, and in this compositional regime, the addition of more antimony does in-

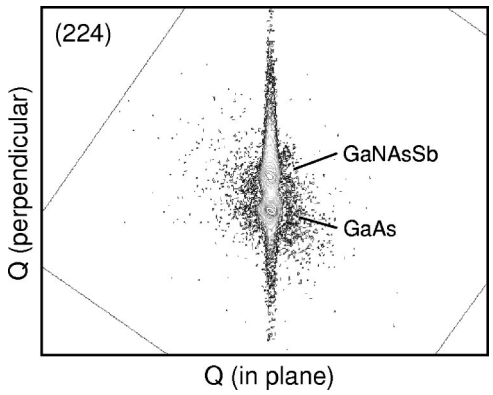

FIG. 3. (224) reciprocal space map of the GaNAsSb sample with 1.0×10^{-8}-Torr BEP Sb.

TABLE I. Summary of GaNAs(Sb) compositions obtained from SIMS, antimony flux used, and strain determined from HRXRD.

Sb BEP (Torr)	N (%)	Sb (%)	Strain
0	0.63	0	−0.13%
1×10^{-8}	0.71	0.6	−0.10%
2×10^{-8}	0.8	1.4	−0.03%
2.8×10^{-8}	0.91	2.0	−0.005%

crease the efficiency with which nitrogen incorporates; the increase in nitrogen is roughly linear with the antimony flux and composition. A previous study with larger antimony fluxes showed only a constant multiplicative enhancement of nitrogen with varying antimony fluxes.[14] Also, the rate at which the enhancement occurs is much higher than previously observed by Harmand *et al.*[15] In the low antimony concentration regime, the enhanced nitrogen incorporation behavior can be fitted to the following linear relationship:

$$\frac{[\mathrm{N}]}{[\mathrm{N}_o]} = K[\mathrm{Sb}] + 1, \tag{1}$$

where $[\mathrm{N}]$ is the nitrogen concentration, $[\mathrm{N}_o]$ is the nitrogen concentration without antimony present, $[\mathrm{Sb}]$ is the antimony concentration in percent, and K is a constant representing the incorporation enhancement. The samples in this work had a much higher enhancement of $K=0.21$ compared to the value of $K=0.03$ reported by Harmand *et al.* It is possible that the rise in nitrogen incorporation efficiency is a rapid phenomenon for small amounts of antimony and levels off to a smaller value with antimony concentrations greater than ~5%. It is clear that antimony does have a significant effect on nitrogen incorporation in the Sb=0%–2% range.

Figure 4 shows the ER spectra measured at 80 K for the set of GaNAsSb layers in the vicinity of the band-gap energy. The $GaN_{0.0063}As_{0.9937}$ layer is under tensile strain, hence two well-separated ER resonances related to absorption between the light-hole (LH) and heavy-hole (HH) valence bands and the conduction band are clearly visible in the ER spectrum in Fig. 4. In addition, signals below the band-gap energy (open circles in Fig. 4) are visible. These oscillations could be associated with the Franz–Keldysh effect which cannot be completely neglected for these layers. It has been concluded that the GaAs buffer layer and GaNAsSb layers are under a significant built-in electric field due to the small thickness of the layers and *n*-type doping in GaAs substrate. In the case of the GaAs buffer layer, the presence of the built-in electric field has been confirmed by the observation of GaAs-related Franz–Keldysh oscillations (FKOs) not shown here.[17] Because both layers are undoped, we conclude that the GaNAsSb layer also has a built-in electric field and the ER wing is most likely associated with this field.

In order to determine the energy of ER resonances, we used the well-known Aspnes third derivative functional form[18] (TDFF)

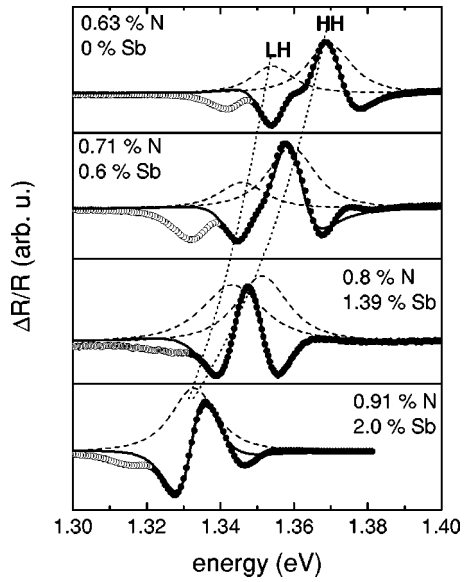

FIG. 4. ER spectra of GaNAs(Sb) layers measured at 80 K with simulated fits. Experimental data are plotted by the open and solid circles. The open circles were neglected during the fitting procedure. The solid lines represent the simulation. The dashed lines represent modulus of individual resonance associated with the LH- and HH-related transitions.

$$\frac{\Delta R}{R} = \mathrm{Re}[Ce^{i\theta}(E - E_0 + i\Gamma)^{-n}], \tag{2}$$

where C is the amplitude, θ the phase angle, E the photon energy, E_0 the transition energy, Γ the broadening parameter, and n the exponent which depends on the type of critical point (we assumed that $n=3$). This formula is the most appropriate for the low-field limit, however, we can use it to determine the energy of ER resonances because FKOs are not observed for the GaNAsSb-related signal.

On the basis of the fitting procedure, the splitting between the LH and HH bands is ~15 meV for $GaN_{0.0063}As_{0.9937}$. With the increase in the incorporation of antimony into the GaNAs layer, the tensile strain decreases to almost zero, as shown in Table I. According to the change in strain, the splitting between LH- and HH-related resonances decreases. The evolution of the valence-band splitting is shown in Fig. 5. Since all the layers in this study were under tensile strain, the fundamental transition is between the LH band and the conduction band. In the case of the sample with the lowest strain, the $GaN_{0.0091}As_{0.9709}Sb_{0.02}$ layer, ER

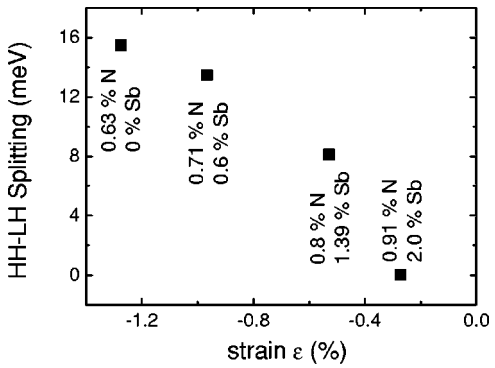

FIG. 5. The valence-band splitting vs the strain in the GaNAs(Sb) layer.

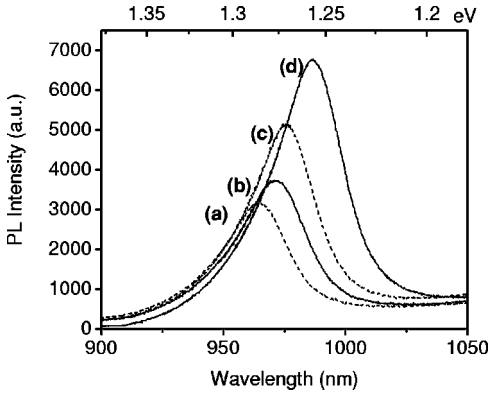

FIG. 6. PL spectra of the GaNAs(Sb) samples showing a redshift and increase in intensity with increasing antimony flux. (a) $GaN_{0.0063}As_{0.9937}$, (b) $GaN_{0.0071}As_{0.9869}Sb_{0.006}$, (c) $GaN_{0.008}As_{0.978}Sb_{0.014}$, and (d) $GaN_{0.0091}As_{0.9709}Sb_{0.02}$.

resonances related to LH and HH transitions are not resolved because the strain values are very small. Therefore, this spectrum could be fitted with only one resonance and explains why the splitting is zero at a finite value of strain.

PL measurements were made at room temperature on as-grown samples using a frequency-doubled diode-pumped yttrium aluminum garnet (YAG) laser at 532 nm to determine the optical qualities and properties of the GaNAs(Sb) layers. As shown in Fig. 6, the position of the $GaN_{0.0063}As_{0.9937}$ layer peak was 964 nm. With the addition of antimony to the GaNAs layer, the peak intensity increased and the wavelength redshifted with increasing antimony flux. The shift in the peak wavelength (out to 987 nm in the $GaN_{0.0091}As_{0.9709}Sb_{0.02}$ sample) was not surprising as the addition of antimony to GaAs reduces the band gap in the GaAsSb alloy. In addition, antimony enhanced the incorporation of nitrogen, which further reduced the band gap. The reduction in band gap agrees with the reduction in transition energy seen in ER. Interestingly, we observed an increase in PL intensity with increasing amounts of nitrogen and antimony in the layer. We previously reported that adding 8%–10% antimony to GaNAs degraded the optical quality of the material even though the addition of antimony to GaInNAs improved the material.[14] These results indicate that the amount of antimony plays a crucial role in whether or not it improves the material. The $GaN_{0.0091}As_{0.9709}Sb_{0.02}$ sample shows $\sim 2.3\times$ increase in PL intensity over the $GaN_{0.0063}As_{0.9937}$ sample as well as a reduction of the full width at half maximum (FWHM) from 56 to 44 meV. It was previously believed that the addition of nitrogen degrades the electronic and optical properties of the material. We show that the addition of small amounts of antimony negates the "nitrogen penalty" and material with more nitrogen can be grown with comparable or better optical quality. Annealed samples were also studied. Although an in-depth discussion is beyond the scope of this paper, those samples had uniformly increased intensity as well as the typical blueshift found in dilute nitrides, but the trends were identical to those in the as-grown samples. With increasing nitrogen content and antimony content, the optical properties have improved. The improvement of GaNAs with increasing amounts of nitrogen and antimony shows that the nitrogen penalty should be thought of as a "nitrogen complexity" in which the optimal growth parameters must be rediscovered for each composition of the alloy.

IV. DISCUSSION

The mechanism of material improvement upon addition of antimony to GaNAs is not completely known. One prominent theory to explain why the addition of antimony to GaNAs improves the material is isoelectronic codoping.[19] Charge codoping in semiconductors allows for greater solubility of the dopants. In a similar manner, isoelectronic codoping in semiconductors should result in the same advantages. The solubility of the isoelectronic species and the carrier mobility should be enhanced. This phenomenon was observed with the increased nitrogen incorporation efficiency. Also, PL intensity improved with increasing nitrogen and antimony concentrations. In isoelectronic codoping, the large antimony atom added to GaNAs compensates the large mismatch in size and electronegativity between the arsenic and nitrogen atoms and leads to defect reduction. A similar behavior has been observed in the GaPNBi system.[20] However, it is uncertain if this is the only effect occurring. As mentioned earlier, antimony was used as a surfactant in GaInNAs to improve material quality. However, what exactly the "surfactant effect" entails is unknown. Surfactant growth itself is still not well understood and is evident from the fact that there are several competing models which describe the mechanisms of improved quality.[21–26] Also, it is possible that the surfactant effect encompasses several effects which all enhance the material quality. Isoelectronic codoping appears to be a model, in this situation, which can explain the improvement in material. However, it is unclear why a much smaller antimony flux is required to improve the material compared to GaInNAs. An order-of-magnitude larger antimony incorporation results in a degradation of GaNAs material. It is possible that adding too much antimony negates isoelectronic codoping effects and degrades GaNAs growth kinetics.

V. SUMMARY

In conclusion, we grew a series of GaNAs(Sb) samples to study the codoping effects of nitrogen and antimony in GaAs. Using SIMS we have determined the compositions of the four samples and discovered that, for a fixed nitrogen flux, the nitrogen concentration increases with increasing antimony concentration. For small amounts of antimony ($<2\%$), the incorporation efficiency of nitrogen with antimony was also observed to be much higher than previously reported values. HRXRD was used to determine the strain in the layers and to confirm that the material was of good structural quality. ER spectra provided information on the band properties of the GaNAs(Sb) layers and also showed a valence-band evolution which agreed with the strain measured from HRXRD. PL measurements indicated an improvement in optical quality with increasing nitrogen and antimony concentrations. A redshift in the wavelength due to increased amounts of nitrogen and antimony also agreed

with the shift in transition energies measured in ER. Isoelectronic codoping can explain why the addition of antimony to GaNAs improves the material quality. Further study is required to understand the behavior of antimony and nitrogen incorporation more completely. Antimony compositions above 2% and below 10% need to be examined to determine the optimal growth parameters of GaNAsSb for good optical quality and to examine the different behaviors of antimony in different amounts.

ACKNOWLEDGMENTS

One of the authors (H.Y.) would like to thank the Stanford Graduate Fellowships for funding assistance. This work was supported under DARPA and ARO contracts MDA972-00-1-024, DAAD17-02-C-0101, and DAAD199-02-1-0184, ONR contract N00014-01-1-00100, High-Power Laser MURI contract, and the Stanford Network Research Center (SNRC).

[1]M. Kondow, K. Uomi, A. Niwa, T. Kitatani, S. Watahiki, and Y. Yazawa, Jpn. J. Appl. Phys., Part 1 **35**, 1273 (1996).
[2]M. Weyers, M. Sato, and H. Ando, Jpn. J. Appl. Phys., Part 2 **31**, L853 (1992).
[3]M. C. Larson, C. W. Coldren, S. G. Spruytte, H. E. Petersen, and J. S. Harris, Jr., IEEE Photon. Technol. Lett. **12**, 1598 (2000).
[4]N. Tansu, N. J. Kirsch, and L. J. Mawst, Appl. Phys. Lett. **81**, 2523 (2002).
[5]R. Johnson *et al.*, Proc. SPIE **4994**, 222 (2003).
[6]P. Krispin, V. Gambin, J. S. Harris, and K. H. Ploog, J. Appl. Phys. **93**, 6095 (2003).
[7]V. Gambin, W. Ha, M. A. Wistey, H. B. Yuen, S. R. Bank, S. M. Kim, and J. S. Harris, Jr., IEEE J. Sel. Top. Quantum Electron. **8**, 795 (2002).
[8]M. Copel, M. C. Reuter, E. Kaxiras, and R. M. Tromp, Phys. Rev. Lett. **63**, 632 (1989).
[9]X. Yang, M. J. Jurkovic, J. B. Heroux, and W. I. Wang, Appl. Phys. Lett. **75**, 178 (1999).
[10]H. Shimizu, K. Kumada, S. Uchiyama, and A. Kasukawa, Electron. Lett. **36**, 1379 (2000).
[11]X. Yang, J. B. Heroux, L. F. Mei, and W. I. Wang, Appl. Phys. Lett. **78**, 4068 (2001).
[12]S. R. Bank, M. A. Wistey, L. L. Goddard, H. B. Yuen, V. Lordi, and J. S. Harris, IEEE J. Quantum Electron. **40**, 656 (2004).
[13]M. A. Wistey, S. R. Bank, H. B. Yuen, L. L. Goddard, and J. S. Harris, Jr., Electron. Lett. **39**, 1822 (2003).
[14]H. B. Yuen, S. R. Bank, M. A. Wistey, A. Moto, and J. S. Harris, Jr., J. Appl. Phys. **96**, 6375 (2004).
[15]J. C. Harmand, G. Ungaro, L. Largeau, and G. LeRoux, Appl. Phys. Lett. **77**, 2482 (2000).
[16]K. Volz, V. Gambin, W. Ha, M. A. Wistey, H. B. Yuen, S. R. Bank, and J. S. Harris, Jr., J. Cryst. Growth **251**, 360 (2003).
[17]F. H. Pollak, in *Modulation Spectroscopy of Semiconductors and Semiconductor Microstructures*, Handbook on Semiconductors, Vol. 2, edited by T. S. Moss (Elsevier Science, Amsterdam, 1994), pp. 527–635.
[18]D. E. Aspnes, Surf. Sci. **37**, 418 (1973).
[19]A. Mascarenhas, Y. Zhang, J. Verley, and M. J. Seong, Superlattices Microstruct. **29**, 395 (2001).
[20]K. Oe and H. Okamoto, Jpn. J. Appl. Phys., Part 2 **37**, L1283 (1998).
[21]R. L. Schwoebel, J. Appl. Phys. **40**, 614 (1969).
[22]G. Erlich and F. G. Hudda, J. Chem. Phys. **44**, 1039 (1966).
[23]E. Tournie and K. H. Ploog, Thin Solid Films **231**, 43 (1993).
[24]J. Massies and N. Grandjean, Phys. Rev. B **48**, 8502 (1993).
[25]B. Voigtlander, A. Zinner, T. Weber, and H. P. Bonzel, Phys. Rev. B **51**, 7583 (1995).
[26]D. Kandel and E. Kaxiras, Phys. Rev. Lett. **75**, 2742 (1995).